Research Article | Vol. 8, No. 7 | 1 Jul 2017 | BIOMEDICAL OPTICS EXPRESS 3410
Biomedical Optics EXPRESS

Temporal multiplexing to simulate multifocal intraocular lenses: theoretical considerations

VYAS AKONDI,[1,*] CARLOS DORRONSORO,[1] ENRIQUE GAMBRA,[1,2] AND SUSANA MARCOS[1]

[1] *Visual Optics and Biophotonics Laboratory, Instituto de Óptica, CSIC, Madrid, Spain*
[2] *2Eyes Vision SL, Madrid, Spain*
[*] *vyas.akondi@io.cfmac.csic.es*

Abstract: Fast tunable lenses allow an effective design of a portable simultaneous vision simulator (SimVis) of multifocal corrections. A novel method of evaluating the temporal profile of a tunable lens in simulating different multifocal intraocular lenses (M-IOLs) is presented. The proposed method involves the characteristic fitting of the through-focus (TF) optical quality of the multifocal component of a given M-IOL to a linear combination of TF optical quality of monofocal lenses viable with a tunable lens. Three different types of M-IOL designs are tested, namely: segmented refractive, diffractive and refractive extended depth of focus. The metric used for the optical evaluation of the temporal profile is the visual Strehl (VS) ratio. It is shown that the time profiles generated with the VS ratio as a metric in SimVis resulted in TF VS ratio and TF simulated images that closely matched the TF VS ratio and TF simulated images predicted with the M-IOL. The effects of temporal sampling, varying pupil size, monochromatic aberrations, longitudinal chromatic aberrations and temporal dynamics on SimVis are discussed.

OCIS codes: (330.0330) Vision, color, and visual optics; (330.7327) Visual optics, ophthalmic instrumentation; (330.5370) Physiological optics; (220.1010) Aberrations (global); (220.1080) Active or adaptive optics.

References and links

1. C. Buznego and W. B. Trattler, "Presbyopia-correcting intraocular lenses," Curr. Opin. Ophthalmol. **20**(1), 13–18 (2009).
2. C. Dorronsoro, A. Radhakrishnan, J. R. Alonso-Sanz, D. Pascual, M. Velasco-Ocana, P. Perez-Merino, and S. Marcos, "Portable simultaneous vision device to simulate multifocal corrections," Optica **3**(8), 918–924 (2016).
3. P. de Gracia, C. Dorronsoro, A. Sánchez-González, L. Sawides, and S. Marcos, "Experimental Simulation of Simultaneous Vision," Invest. Ophthalmol. Vis. Sci. **54**(1), 415–422 (2013).
4. S. Manzanera, P. M. Prieto, D. B. Ayala, J. M. Lindacher, and P. Artal, "Liquid crystal Adaptive Optics Visual Simulator: Application to testing and design of ophthalmic optical elements," Opt. Express **15**(24), 16177–16188 (2007).
5. J. D. Marsack, L. N. Thibos, and R. A. Applegate, "Metrics of optical quality derived from wave aberrations predict visual performance," J. Vis. **4**(8), 322–328 (2004).
6. V. Akondi, P. Pérez-Merino, E. Martinez-Enriquez, C. Dorronsoro, N. Alejandre, I. Jiménez-Alfaro, and S. Marcos, "Evaluation of the true wavefront aberrations in eyes implanted with a rotationally asymmetric multifocal intraocular lens," J. Refract. Surg. **33**(4), 257–265 (2017).
7. H. Liou and N. A. Brennan, "Anatomically accurate, finite model eye for optical modeling," J. Opt. Soc. Am. A **14**(8), 1684–1695 (1997).
8. J. Schwiegerling, *Field Guide to Visual and Ophthalmic Optics* (SPIE Press, 2004).
9. L. N. Thibos, X. Hong, A. Bradley, and R. A. Applegate, "Accuracy and precision of objective refraction from wavefront aberrations," J. Vis. **4**(4), 329–351 (2004).
10. M. J. Kim, L. Zheleznyak, S. MacRae, H. Tchah, and G. Yoon, "Objective evaluation of through-focus optical performance of presbyopia-correcting intraocular lenses using an optical bench system," J. Cataract Refract. Surg. **37**(7), 1305–1312 (2011).
11. J. Schwiegerling, "Statistical generation of normal and post-refractive surgery wavefronts," Clin. Exp. Optom. **92**(3), 223–226 (2009).
12. M. B. Roopashree, V. Akondi, S. J. Weddell, and R. P. Budihal, "Myopic aberrations: Simulation based comparison of curvature and Hartmann Shack wavefront sensors," Opt. Commun. **312**(1), 23–30 (2014).
13. V. Akondi and B. Vohnsen, "Myopic aberrations: impact of centroiding noise in Hartmann Shack wavefront sensing," Ophthalmic Physiol. Opt. **33**(4), 434–443 (2013).
14. W. N. Charman and J. A. M. Jennings, "Objective measurements of the longitudinal chromatic aberration of the human eye," Vis. Res. **16**(9), 999–1005 (1976).

#292972 https://doi.org/10.1364/BOE.8.003410
Journal © 2017 Received 17 Apr 2017; revised 7 Jun 2017; accepted 11 Jun 2017; published 23 Jun 2017

Biomedical Optics EXPRESS

15. P. A. Howarth and A. Bradley, "The longitudinal chromatic aberration of the human eye, and its correction," Vis. Res. **26**(2), 361–366 (1986).
16. L. N. Thibos, A. Bradley, D. L. Still, X. Zhang, and P. A. Howarth, "Theory and measurement of ocular chromatic aberration," Vis. Res. **30**(1), 33–49 (1990).
17. J. S. McLellan, S. Marcos, P. M. Prieto, and S. A. Burns, "Imperfect optics may be the eye's defence against chromatic blur," Nature **417**(6885), 174–176 (2002).
18. M. Vinas, C. Dorronsoro, N. Garzon, F. Poyales, and S. Marcos, "In vivo subjective and objective longitudinal chromatic aberration after bilateral implantation of the same design of hydrophobic and hydrophilic intraocular lenses," J. Cataract Refract. Surg. **41**(10), 2115–2124 (2015).
19. M. S. Millan, F. Vega, and I. Rios-Lopez, "Polychromatic image performance of diffractive bifocal intraocular lenses: longitudinal chromatic aberration and energy efficiency," Invest. Ophthalmol. Vis. Sci. **57**(4), 2021–2028 (2016).
20. M. Vinas, A. Gonzalez-Ramos, C. Dorronsoro, V. Akondi, N. Garzon, F. Poyales, and S. Marcos, "In vivo measurement of longitudinal chromatic aberration with multifocal diffractive intraocular lenses," Invest. Ophthalmol. Vis. Sci. (2017, in press).
21. D. Gatinel and Y. Houbrechts, "Comparison of bifocal and trifocal diffractive and refractive intraocular lenses using an optical bench," J. Cataract Refract. Surg. **39**(7), 1093–1099 (2013).
22. S. Marcos, S. A. Burns, E. Moreno-Barriusop, and R. Navarro, "A new approach to the study of ocular chromatic aberrations," Vis. Res. **39**(26), 4309–4323 (1999).

1. Introduction

Presbyopia is the loss of good near vision that affects middle and old-aged population. The blurring of near vision is due to a reduced elasticity of the crystalline lens. Simultaneous vision can be provided in the form of several multifocal solutions (contact lenses, intraocular lenses or corneal treatment) for presbyopia correction [1]. Multifocal intraocular lenses (M-IOLs) provide concurrent vision in focus at two or more distances. M-IOL replaces the crystalline lens in a cataract surgery providing the patient with good vision at near and far distances (besides adequate intermediate vision with certain M-IOLs). It can be difficult for a surgeon to describe the visual benefit and possible visual outcomes of the surgery to a patient when a specific M-IOL is implanted. In addition, there are many multifocal solutions available in the market and it is complicated for the surgeon to identify the most suitable multifocal correction for a given patient [2]. An instrument that provides the visual experience of simultaneous vision to the patient before the surgery can be useful.

A simultaneous vision simulator (SimVis) allows prospective cataract surgery patients to experience multifocal vision with several M-IOLs, evaluate the visual benefit quantitatively and then choose the best solution for their needs [3, 4]. SimVis based on a tunable lens has proven its potential in building a compact device that can provide a realistic and wide field of view optical simulation of the visual experience offered by M-IOLs [2]. The tunable lens allows temporal multiplexing and generates fast periodic foci variations at speeds greater than the flicker fusion threshold of the human visual system. With such a system, seemingly static images as seen through a multifocal correction can be constructed on an observer's retina. Commercial M-IOL designs can be envisioned with the tunable lens based SimVis device by evaluating the corresponding temporal profile of the focal distance in a tunable lens that results in a through-focus (TF) optical quality equal to the TF optical quality of the M-IOL.

In this paper, for the first time, a method is proposed to evaluate the temporal profile (in a SimVis based on a tunable lens) corresponding to the multifocal component of any given M-IOL. Its application is demonstrated in simulating three different commercial intraocular lens designs. The proposed metric-based evaluation of the temporal profile uses TF Visual Strehl (VS) ratio based on the optical transfer function (OTF) [5]. The goodness of the approach is confirmed by means of TF simulated images and a 2-D correlation metric obtained for both the real M-IOL and the proposed temporal multiplexing approach.

Biomedical Optics EXPRESS

2. Method

The fundamental principle behind the simulation of the M-IOLs with a tunable lens is associated with the conversion of the spatially varying pupillary power distribution of a given M-IOL to a time-varying focus distribution. For example, in the simple case of a segmented bifocal phase pattern with well-defined 1:1 energy ratio for far (0 D) and near (3 D) distances, there are distinctly two focusing distances. Consequently, the corresponding SimVis time coefficients for the tunable lens in creating the two distinct foci with 0 D and 3 D are in the ratio 1:1. One-half of the time in a single SimVis cycle is spent in generating the far focus and the remaining half for the near focus. However, visual identification of the distinct foci and their corresponding energies from the phase maps is not possible with most designs of commercial M-IOLs. Also, the energy distribution at different distances could be dependent on wavelength and pupil size.

Here, a new method is described that uses the TF VS ratio as a reference metric to evaluate the time coefficients for SimVis corresponding to any given M-IOL. This is done by evaluating the phase maps corresponding to the M-IOLs as described in Section 2.1. The following sections, 2.2 – 2.6, describe the proposed method of calculating the temporal profile for SimVis with the help of the TF VS ratio corresponding to any given M-IOL, the means of optimizing the sampling procedure, the metrics used for assessing the performance of the obtained SimVis temporal profile, methods of simulating the effects of aberrations and typical tunable lens specifications.

2.1. Evaluation of the M-IOL phase maps

The phase maps corresponding to the three M-IOLs under consideration were calculated using Zemax software by taking the difference between the phase evaluated in a pseudophakic computer eye model with the M-IOL [6] and an emmetropic eye model with the crystalline lens. It was later verified that by placing the resultant phase map in the pupil plane of an emmetropic eye model with the crystalline lens or the pseudophakic eye model with the M-IOL generated the same TF optical quality. In this paper, the phase maps were evaluated at 555 nm wavelength, unless mentioned otherwise.

Here, the eye model of Liou and Brennan [7] was used as the starting point for evaluating the multifocal phase map due to the M-IOLs. However, it was found that the extracted phase map is independent of the eye model used, as was verified with the Arizona eye model [8]. This was expected because the extracted phase map was due to the power distribution of the M-IOL alone and the spherical aberration in an emmetropic eye model was subtracted from the total phase map. The corneal aberrations were not included in the estimation of the phase map.

The three M-IOLs included in the study were: a bifocal refractive segmented with rotational asymmetry, a trifocal diffractive and a refractive extended depth of focus (EDOF).

2.2. Calculating the time coefficients

The SimVis temporal profile was evaluated by fitting the TF optical quality metric (q - a vector of length 'm') of a given M-IOL with TF optical quality of 'n' monofocal lenses (thin lenses under paraxial approximation) of different addition/defocus (Q - a matrix of dimensions m × n) temporally viable with a tunable lens and using the method of least squares (with non-negativity constraints). Each coefficient in 'm' corresponds to a TF position in diopters. The system of linear equations that relates the TF optical quality of the real M-IOL and the TF optical quality of 'n' monofocal lenses can be written as follows:

$$q = \sum_{i=1}^{n} (a_i) \cdot (Q_i) \tag{1}$$

where, 'a' represents a vector of dimensionless TF optical quality fitting coefficients of length 'n' (each coefficient corresponds to a single monofocal lens). These coefficients, a_i are directly

Biomedical Optics EXPRESS

related to the time spent in each focal length, t_i, by the tunable lens as shown below:

$$\frac{a_i}{\sum a_i} = k\frac{t_i}{\sum t_i}. \tag{2}$$

Using Eq. (2) and substituting a_i in Eq. (1) for a large sampling, n, q can be expressed as follows:

$$q = k \cdot \left(\frac{\sum a_i}{\sum t_i}\right) \cdot \sum_{i=1}^{\mathrm{n}} (t_i) \cdot (Q_i) \tag{3}$$

In this paper, Q_i represents the TF optical quality of n = 161 monofocal lenses that can be generated with the tunable lens and determined over a range of addition: -2 D to +6 D in steps of 0.05 D. Initial sampling with a lower resolution leads to inaccuracies in representing the true TF optical quality of the real M-IOL with SimVis. The TF optical quality (in terms of the metric used for evaluating the time coefficients) of each of these monofocal lenses and the M-IOL was computed over the same range -2 D to +6 D in steps of 0.05 D such that the total number of steps, m = 161. Thus, Q is a matrix of dimensions m × n (161 × 161) and q is a vector with n = 161 elements. The value of n was chosen such that it is much greater than the number of nonzero time coefficients obtained after the fitting (Eq. (3)). The dimensionless proportionality constant, k, tends to unity as sampling increases.

The evaluated SimVis time coefficients, t_i, depend on the choice of the pupil diameter as shown in Section 3.3. This study used a pupil diameter of 4 mm, unless mentioned otherwise.

2.3. Sampling

The number of time samples was set to a high value (n = 161) while determining the temporal profile to retain accuracy. Sampling can be reduced by eliminating time coefficients close to zero. This helps in overcoming time delays in generating foci that insignificantly contribute to simulating the M-IOL's TF optical quality with SimVis. This step is also useful in reducing the total time, $\sum t_i$, spent in a single SimVis cycle, below the flicker fusion threshold of the visual system. Sampling can be reduced by downsampling at regular intervals, thresholding or by selectively picking the time coefficients around relevant additions.

A SimVis cycle needs to be shorter than 40 ms to realize a frame rate better than 25 Hz (as in a standard-definition television). Further, the finite settling time of the tunable lens (typically lower than 5 ms) to fully change between any two foci causes inaccuracies in replicating the TF optical quality. Hence, it is important to utilize the available time reasonably in order to meticulously simulate the prescribed multifocal TF performance with the tunable lens.

The method used for undersampling was different for M-IOLs with distinct TF VS ratio peaks and for those with an EDOF. In the case of undersampling in M-IOLs with distinct TF optical quality peaks, the sampling points at the location of the peaks (far, near and intermediate) were chosen first. Next, based on the full-width-half-maxima of the peaks, additional sampling points were selected around the peak location starting with the next highest time coefficient and so on. In the case of M-IOLs with an EDOF, distinct foci are not expected and hence thresholding was applied directly. In addition, the time coefficients at the sampling points outside the desired addition range provided by the M-IOL were deliberately set to zero.

To simulate multifocal vision, in a single SimVis cycle (shorter than the flicker fusion threshold of human vision), the tunable lens quickly varies its focus covering all the sampling points and the time spent in each focal distance is determined by the evaluated temporal profile. This cycle is repeated several times to display seemingly static images at the retina. Using the same principle, the TF optical quality metric, q_s, as seen by an observer with the SimVis based on the tunable lens was predicted by integrating the weighted point spread functions (PSFs) of the monofocal lenses simulated with the tunable lens over a single SimVis cycle. Here, weighting was done with the help of the determined time coefficients, t_i (in Eq. (3)), or the undersampled time coefficients,

Biomedical Optics EXPRESS

$t_{s,i}$, which were obtained by setting to zero the time coefficients in 't' that do not contribute considerably to 'q' (applying thresholding, making q_s an approximation of q). In general, the number of nonzero time coefficients (n_{SimVis}) in t_s is much lower than the total sampling, n = 161. Here, q_s is a vector of length 'n'.

The accuracy of a given SimVis temporal sampling can be quantified with the help of $\tilde{q}$, which is the relative error in the optical quality, and is defined as follows:

$$\tilde{q} = \frac{1}{n}\sum_{j=1}^{n}\left|\frac{q_j - q_{s,j}}{q_j}\right| \tag{4}$$

The mean value, $\tilde{q}$, gives a point-wise correspondence between the two vectors, q and q_s such that the value of $\tilde{q}$ is zero (ideal situation) when q and q_s are identical and $\tilde{q}$ is unity when all the time coefficients are zero.

2.4. Through-focus optical quality metrics

In this paper, the TF optical quality vector, 'q', was determined with the TF VS ratio as the metric. This was calculated for the three different M-IOLs by applying fast Fourier transform (FFT) calculations on the M-IOL phase maps (Section 2.1). The accuracy with which the tunable lens (temporal profile with a given sampling) replicates the TF optical performance of a given M-IOL was evaluated with the help of the following two evaluation metrics for SimVis:

- TF VS ratio
- TF simulated images and 2-D image correlation coefficients.

The SimVis TF optical quality vector, q_s corresponding to the three M-IOLs was then evaluated and compared with 'q' obtained with the M-IOL. The VS ratio is representative of the optical quality of the lens and is defined as follows [9]:

$$\text{VS ratio} = \frac{\iint_{-\infty}^{\infty} C(x',y')\cdot O(x',y')dx'dy'}{\iint_{-\infty}^{\infty} C(x',y')\cdot O_{DL}(x',y')dx'dy'}. \tag{5}$$

Here, O denotes the OTF obtained with the M-IOL phase map and O_{DL} is the diffraction limited OTF. And, C is the neural contrast sensitivity function. (x', y') represents the spatial frequency coordinates corresponding to the rectangular cartesian coordinates, (x, y).

The TF simulated images provide a direct comparison of the effect of the evaluated TF PSFs. These images were evaluated for the real M-IOL and SimVis by convolving a nominal image (letter 'E') with the real M-IOL TF PSFs or the SimVis TF PSFs (time integrated over a single SimVis cycle). The TF simulated images were evaluated in the addition range -2.0 D to 5.0 D in steps of 0.1 D. TF 2-D image correlation coefficient was calculated between the nominal image (shown in Fig. 1(d)) and the TF simulated images predicted with the real M-IOL (c) or the SimVis (c_s) based on the tunable lens. The 2-D image correlation coefficient is equal to unity when the two compared images are identical. This metric is known to be reliable in evaluating the visual performance [10].

The evaluated TF 2-D image correlation coefficients offer another relative error metric for optimizing sampling, which is defined by the relative error $\tilde{c}$, such that

$$\tilde{c} = \frac{1}{n}\sum_{j=1}^{n}\left|\frac{c_j - c_{s,j}}{c_j}\right|. \tag{6}$$

Here, c and c_s are vectors of length 'n'. Root-mean-square (RMS) of the differences q-q_s and c-c_s were also used for comparison of the TF optical quality. In the case of the trifocal diffractive

Biomedical Optics EXPRESS

and segmented bifocal refractive M-IOLs, the RMS was evaluated in the addition range: -0.5 D to 4.0 D and in the case of refractive EDOF M-IOL, the upper bound was reduced to 2.5 D.

2.5. Monochromatic and polychromatic aberrations

Monochromatic aberrations were statistically simulated from the wavefront data of 41 subjects [11, 12]. In this study, 20 different wavefronts were generated. The statistics of the generated representative wavefronts were consistent with the covariance statistics of Zernike coefficients of the 41 subjects [13].

The human eye exhibits longitudinal and transverse chromatic aberrations arising from the cornea and the ocular media [15–17]. The implanted M-IOL introduces noticeable pseudophakic longitudinal chromatic aberration (LCA), which arises due to the chromatic dispersion of the M-IOL materials [18]. Refractive M-IOLs introduce LCA due to refraction alone. In the case of diffractive M-IOLs, along with the refractive LCA, an additional LCA due to diffraction is introduced [19–21]. Diffractive M-IOLs lenses are usually designed such that the diffractive LCA fully or partially compensates the refractive LCA at near and intermediate distances. The presence of LCA causes a dependence of TF optical quality with wavelength.

Polychromatic image quality metrics are needed to apprehend human vision with polychromatic stimuli. Further, polychromatic TF VS ratio can be obtained by integrating monochromatic TF PSFs weighted by the Commission Internationale de L'Eclairage (CIE) standard relative photopic spectral sensitivity [22]. The CIE spectral sensitivity data was precisely fitted to three significant digits using the first nine terms of the Fourier series expansion. The phase maps corresponding to different wavelengths (visible range) in steps of 10 nm were obtained in pseudophakic computer eye models. TF PSFs corresponding to the phase maps at each wavelength were estimated. The polychromatic TF VS ratio was evaluated from a summation of the obtained TF PSFs weighted with the spectral sensitivity at each wavelength.

2.6. Typical tunable lens specifications

SimVis can be realized by using an optical liquid filled lens that allows optomechanical tunability in focus at a rate faster than 200 Hz [2]. The settling time, which is the time taken by the device to fully change from one focus state to another is lower than 5 ms when the maximum power difference between the two generated foci is 3 D. Recent commercial designs of these lenses reduce thermal drift effects (changes in optical power with varying temperature) and the wavefront error is usually in the range of 0.12-0.27 μm for a 10 mm active aperture diameter at 555 nm. The proposed method of evaluating the time coefficients for SimVis does not take into consideration the dynamic behavior of the tunable lenses, the wavefront aberrations introduced by the lens and the thermal drift effects. However, with an appropriate calibration of the tunable lens, a correction to the resultant time coefficients is possible to replicate the TF profiles of the M-IOL with reasonable accuracy.

3. Results

The proposed method was applied to trifocal diffractive, segmented bifocal refractive and refractive EDOF M-IOLs. The phase maps of these M-IOLs were evaluated using ray tracing based pseudophakic computer eye models and the TF optical quality of the phase maps was computed using FFT methods. The SimVis time coefficients corresponding to the M-IOLs were obtained by using Eq. (3). The number of nonzero time coefficients for the segmented bifocal refractive, trifocal diffractive and refractive EDOF M-IOLs was found to be 57, 97 and 116 respectively. Undersampling was then applied to each of the M-IOLs such that they contained a chosen number of nonzero time coefficients, n_{SimVis}. The TF optical quality of SimVis for each M-IOL with the chosen sampling is estimated from the integrated TF PSFs weighted with the time coefficients.

Biomedical Optics EXPRESS

3.1. Application of the proposed method

Figure 1(a) shows a comparison of the TF VS ratio, q, of a trifocal diffractive M-IOL at 555 nm with 4 mm pupil diameter, the TF VS ratio of its SimVis temporal profile obtained with high sampling (n_{SimVis} = 50) and the TF VS ratio, q_s, of a greatly undersampled SimVis (n_{SimVis} = 12, as an example). An excellent point-to-point correspondence was obtained between the TF VS ratio of the real M-IOL and the TF VS ratio of the SimVis with high sampling (n_{SimVis} = 50). For an undersampled case (n_{SimVis} = 12), the RMS difference between q and q_s is 0.03. The corresponding undersampled normalized time coefficients, t_s with n_{SimVis} = 12 are shown in Figure 1(b). The maximum value of t_s is at 0 D (as expected the maximum energy is at the far distance). The nonzero time coefficients in a highly undersampled SimVis are mostly confined near the location of the TF VS ratio peaks, spending 58% of a single SimVis cycle in far, 26% in near and 16% in intermediate distance. Figure 1(c) shows a comparison of the TF 2-D correlation vectors c and c_s obtained from the simulated images (n_{SimVis} = 12). Additionally, the TF 2-D image correlation coefficient obtained by calculating the correlation between the SimVis TF simulated images and M-IOL TF simulated images is also shown (in green). Figure 1(d) shows the nominal 'E' image used for convolving with the TF PSFs. Figure 1(e) shows the TF simulated images evaluated with the trifocal diffractive M-IOL and the TF simulated images obtained with the corresponding undersampled SimVis temporal profile (n_{SimVis} = 12).

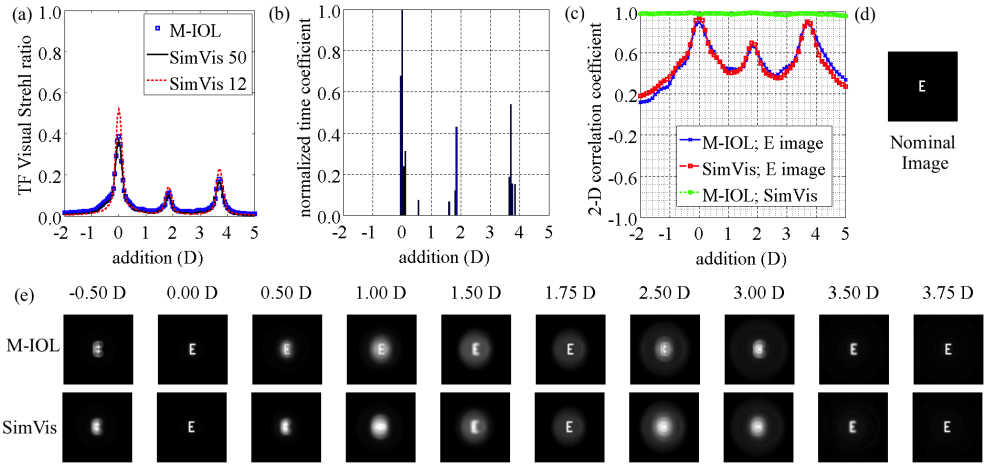

Fig. 1. Trifocal diffractive IOL: (a) Comparison of TF VS ratio of the M-IOL (q) and its SimVis temporal profile, (q_s) for two cases: n_{SimVis} = 50 and n_{SimVis} = 12. (b) The corresponding normalized time coefficients, t_s, when n_{SimVis} = 12. (c) Comparison of the 2-D correlation between the nominal 'E' image and the TF simulated images; simulated images were obtained with either the real M-IOL (c) or the tunable lens based SimVis (c_s) with n_{SimVis} = 12. The 2-D correlation between the TF simulated images obtained with the real M-IOL and SimVis (n_{SimVis} = 12) is also shown. (d) Nominal 'E' image. (e) The TF simulated images obtained with the M-IOL and the SimVis (n_{SimVis} = 12).

Figure 2 is similar to Figure 1 for the segmented bifocal refractive M-IOL with a SimVis undersampling of n_{SimVis} = 7. Here, the RMS difference between q and q_s is 0.01, the maximum value of t_s is at 0 D (as expected the maximum energy is at far distance). Here too, the nonzero time coefficients in a highly undersampled SimVis are confined near the location of the TF VS ratio peaks, spending 56% of a single SimVis cycle in far and 44% in near.

Figure 3 shows the case of the refractive EDOF M-IOL with a SimVis undersampling of n_{SimVis} = 23. For this undersampled case, the RMS difference between q and q_s is 0.02. The corresponding undersampled normalized time coefficients, t_s with n_{SimVis} = 23 are shown in

Biomedical Optics EXPRESS

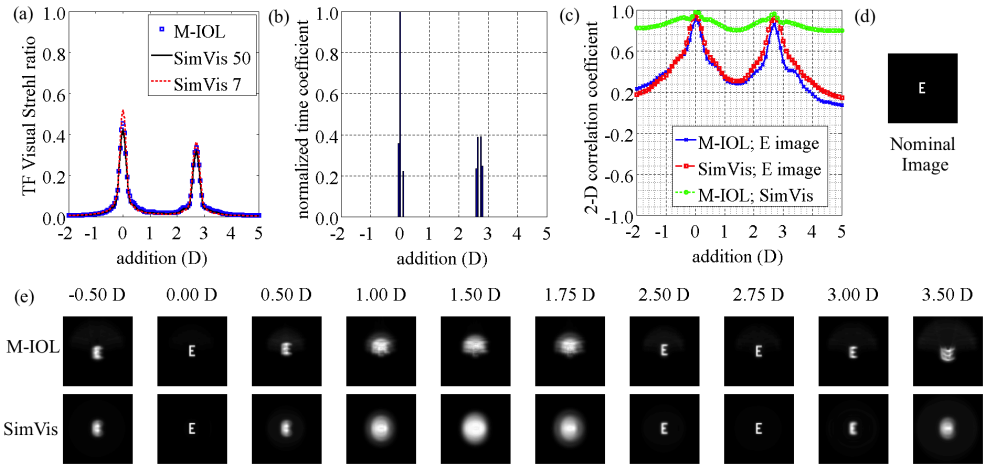

Fig. 2. Segmented bifocal refractive IOL: (a) Comparison of TF VS ratio of the M-IOL (q) and its SimVis temporal profile, (q_s) for two cases: n_{SimVis} = 50 and n_{SimVis} = 7. (b) The corresponding normalized time coefficients, t_s, when n_{SimVis} = 7. (c) Comparison of the 2-D correlation between the nominal 'E' image and the TF simulated images; simulated images were obtained with either the real M-IOL (c) or the tunable lens based SimVis (c_s) with n_{SimVis} = 7. The 2-D correlation between the TF simulated images obtained with the real M-IOL and SimVis (n_{SimVis} = 7) is also shown. (d) Nominal 'E' image. (e) The TF simulated images obtained with the M-IOL and the SimVis (n_{SimVis} = 7).

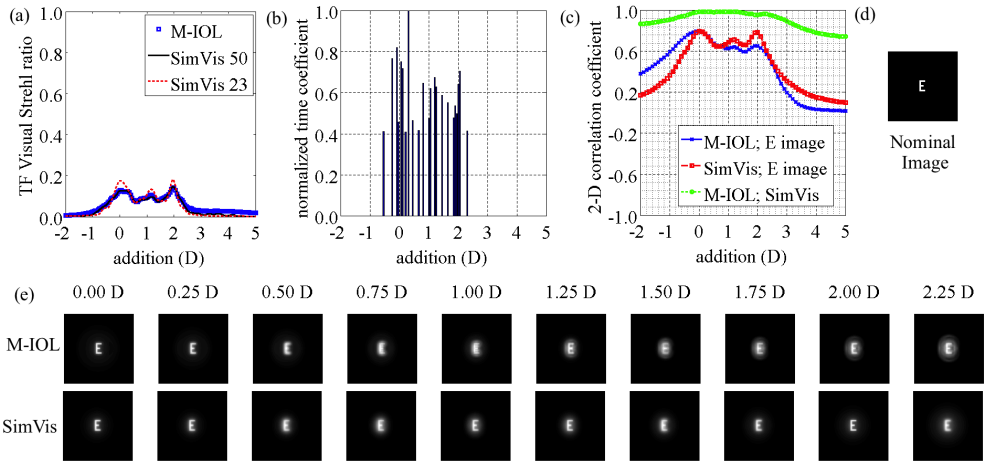

Fig. 3. Refractive EDOF IOL: (a) Comparison of TF VS ratio of the M-IOL (q) and its SimVis temporal profile, (q_s) for two cases: n_{SimVis} = 50 and n_{SimVis} = 23. (b) The corresponding normalized time coefficients, t_s, when n_{SimVis} = 23. (c) Comparison of the 2-D correlation between the nominal 'E' image and the TF simulated images; simulated images were obtained with either the real M-IOL (c_s) or the tunable lens based SimVis (c_s) with n_{SimVis} = 23. The 2-D correlation between the TF simulated images obtained with the real M-IOL and SimVis (n_{SimVis} = 23) is also shown. (d) The TF simulated images obtained with the M-IOL and the SimVis (n_{SimVis} = 23).

Biomedical Optics EXPRESS

Figure 3(b). The maximum value of t_s occurred at an addition of 0.3 D. Due to the absence of distinct peaks in the TF VS ratio for this M-IOL, the nonzero time coefficients in a undersampled SimVis (n_{SimVis} = 23) are spread over a large range of addition: -0.5 D to 2.5 D.

3.2. Optimal sampling

The parameters $\tilde{q}$ (Eq. (4)) and $\tilde{c}$ (Eq. (6)) vary with SimVis sampling for the three M-IOLs examined here as can be seen in Fig. 4. Since TF VS ratio is the metric that is used for evaluating the time coefficients, as expected, the value of $\tilde{q}$ drops with increasing sampling in all the three cases as can be seen in Fig. 4(a). TF image correlation coefficient based metric, $\tilde{c}$, can be used as an indicator of the optimal sampling (see Fig. 4(b)). In the case of a trifocal diffractive M-IOL, $\tilde{q}$ and $\tilde{c}$ have a local minima at n_{SimVis} = 12 and these values do not drop significantly beyond n_{SimVis} = 12 and hence this sampling was chosen as an example in Fig. 1. Similarly, in the case of segmented bifocal refractive IOL, there exists a local minimum for $\tilde{q}$ at n_{SimVis} = 7. The value of $\tilde{c}$ increases beyond this local optimal sampling value based on $\tilde{q}$. In the case of the refractive EDOF M-IOL, $\tilde{q}$ saturates beyond n_{SimVis} = 22, which is higher than the optimal sampling in trifocal diffractive and segmented bifocal refractive M-IOLs. Since $\tilde{c}$ has a local minima at n_{SimVis} = 23, this was chosen as the local optimum sampling in this case.

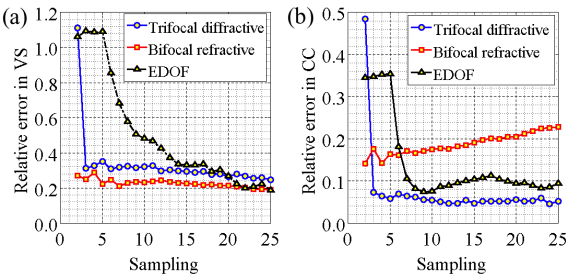

Fig. 4. The effect of sampling on the SimVis temporal profile optimization metric based on: (a) TF VS ratio ($\tilde{q}$, Eq. (4)) and (b) TF 2-D image correlation coefficient ($\tilde{c}$, Eq. (6)).

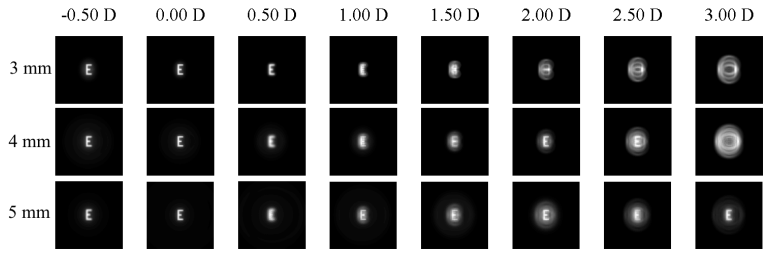

Fig. 5. The effect of pupil diameter variations (at 3 mm, 4mm and 5mm) in terms of the TF simulated images for the EDOF M-IOL.

3.3. Effect of pupil size variations

The evaluated TF VS ratio is pupil size dependent for the case of M-IOLs. Here, the M-IOLs can be distinguished into two kinds. Firstly, those M-IOLs for which the energy distribution for far and near is pupil size-independent, and those that are pupil size-dependent. For the former, diffraction-limited PSFs alone affect TF VS ratio curves with a change in pupil size. Since the corresponding monofocal TF curves also change in the same way with pupil size, the effect of pupil size variations on the SimVis time coefficients should be limited to sampling (see Eq. (3)).

Biomedical Optics EXPRESS

However, for the latter M-IOLs, the pupil size variations play a larger role in determining the TF optical quality. An example of such pupil size variations in terms of the TF simulated images for the EDOF M-IOL is shown in Fig. 5. In these M-IOLs, SimVis time coefficients should be evaluated separately for each pupil size. They can be precomputed and stored for a better operational speed of the SimVis instrument.

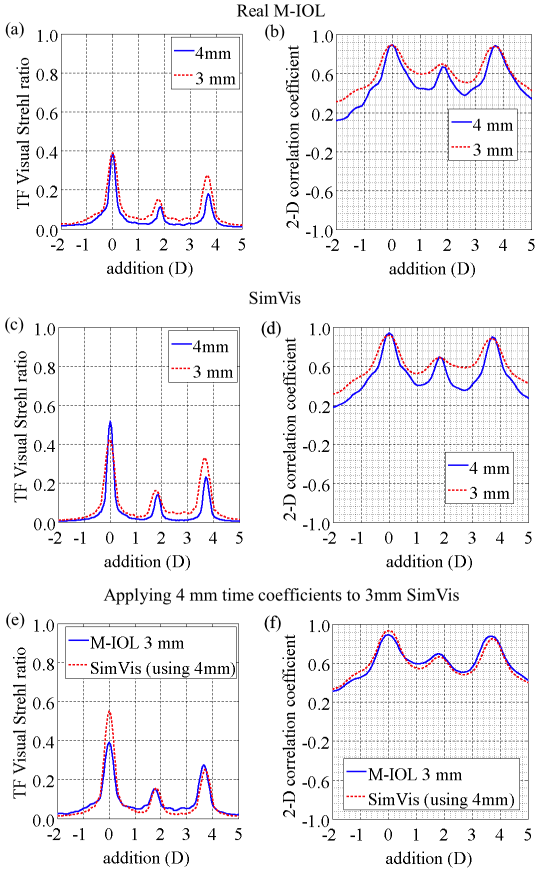

Fig. 6. Effect of pupil size variations in a trifocal diffractive M-IOL: Comparison of the 4 mm and 3 mm pupil diameters in terms of (a) TF VS ratio and (b) TF correlation coefficient for the real M-IOL. Corresponding 4 mm and 3 mm SimVis TF curves (c) VS ratio and (d) correlation coefficient. (e) A comparison of the TF optical quality of the real M-IOL with 3 mm pupil diameter and corresponding SimVis that uses the time coefficients obtained for a 4 mm pupil diameter M-IOL. Here, a sampling of $n_{SimVis} = 12$ was used in a trifocal diffractive M-IOL.

A comparison of the TF VS ratio obtained using predictions of SimVis simulations for a 4 mm pupil diameter and 3 mm pupil diameter are shown in Fig. 6 for the trifocal diffractive M-IOL. Here, a sampling of $n_{SimVis} = 12$ is used. A comparison of the TF optical quality for the trifocal diffractive M-IOL with 4 mm and 3 mm pupil diameters is shown in Figs. 6(a) and 6(b). A comparison of the corresponding SimVis TF profiles is shown in Figs. 6(c) and 6(d). In each case (Figs. 6(a)-6(d)), the 3 mm TF profiles are wider than the 4 mm TF profiles. To comprehend the effect of changes in pupil diameter on SimVis, the SimVis time coefficients obtained using a 4 mm pupil diameter M-IOL phase profile were applied to a SimVis with 3 mm pupil diameter. The effect of a reduced pupil size is shown in Figs. 6(e) and 6(f). The use of 4 mm

Biomedical Optics EXPRESS

pupil diameter SimVis time coefficients in a 3 mm pupil diameter SimVis condition, the RMS error of the difference, q-q_s, increased to 0.05 from 0.03 (see Section 3.1). This error reduced to 0.04 when the sampling was increased to n_{SimVis} = 25. With further increase in sampling, this error due to a change in pupil size remained unaffected at 0.04.

In the case of the segmented bifocal refractive M-IOL (n_{SimVis} = 7), the use of the time coefficients evaluated with a 4 mm pupil diameter M-IOL phase map, in a 3 mm SimVis, resulted in RMS error in the differences, q-q_s and c-c_s, of 0.04 and 0.09 respectively, as illustrated in Figs. 7(a) and 7(b). Increasing the sampling to n_{SimVis} = 25 in the case of segmented bifocal refractive M-IOL reduced the RMS error in the difference, q-q_s, to 0.02, while the RMS error in the difference, c-c_s, remained the same at 0.09.

For the refractive EDOF M-IOL (n_{SimVis} = 23), the use of the time coefficients evaluated with a 4 mm pupil diameter, in a 3 mm SimVis, resulted in a very high RMS error in the differences, q-q_s and c-c_s, of 0.08 and 0.20 respectively as shown in Fig. 7(c) and 7(d). The refractive EDOF M-IOL showed large variations in the TF optical quality with changing pupil size, significantly affecting the SimVis time coefficients.

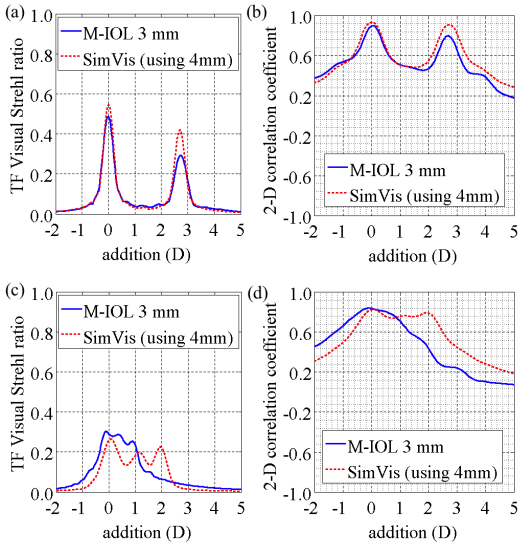

Fig. 7. A comparison of the TF optical quality of the real M-IOL with 3 mm pupil diameter and corresponding SimVis that uses the time coefficients obtained for a 4 mm pupil diameter M-IOL in the case of segmented bifocal refractive M-IOL in terms of (a) TF VS ratio and (b) TF correlation coefficient and in the case of refractive EDOF M-IOL in terms of (c) TF VS ratio and (d) TF correlation coefficient.

3.4. *Wavefront aberrations of the eye and their effects on SimVis*

Higher-order aberrations (HOA) of the eye result in a reduction of the peaks in the TF VS ratio at near, far and intermediate distances. In most cases, there is an observed broadening of the TF optical quality profiles. To analyze the effects of HOA on SimVis, the question to ask here is - Do the wavefront aberrations of the eye affect the TF optical quality of SimVis in the same way as the real M-IOL would? To answer this question, two examples of typical eye's wavefronts (WF 1 and WF 2, statistically generated as described in Section 2.5) were considered. The two aberrated wavefronts, WF 1 and WF 2, within a 4 mm pupil diameter had a peak-to-valley of 0.60 μm and 0.43 μm respectively. And, the corresponding RMS wavefront errors were 0.07 μm and 0.14 μm. WF 1 had a spherical aberration coefficient of 0.01 μm and WF 2 had a spherical aberration

Biomedical Optics EXPRESS

coefficient of 0.06 μm. A comparison was made between the TF optical quality profiles predicted in SimVis and the real M-IOL by including the effects of these wavefront aberrations.

It was found that in the case of the segmented bifocal refractive and trifocal diffractive M-IOLs, the SimVis TF profiles (VS ratio and correlation coefficient) with HOA follow the TF profiles of the real M-IOL with HOA. Figures 8(a)-8(f) show the effect on the TF optical quality due to the WF 1 aberrations, inscribed in Fig. 8(a) with the segmented bifocal refractive, trifocal diffractive and refractive EDOF M-IOLs. Here, a sampling of n_{SimVis} = 7 for segmented bifocal refractive, n_{SimVis} = 12 for trifocal diffractive and n_{SimVis} = 50 for refractive EDOF M-IOLs was chosen. The results for WF 2 are shown in Figs. 8(g)-8(l). The RMS error of the difference in TF optical quality metrics corresponding to real M-IOLs and SimVis is tabulated (see Table 1) for the two aberration cases. The mean RMS of the difference in the TF optical quality (between real M-IOL with aberrations and corresponding SimVis with aberrations) of 20 simulated wavefronts is also shown along with the standard deviation.

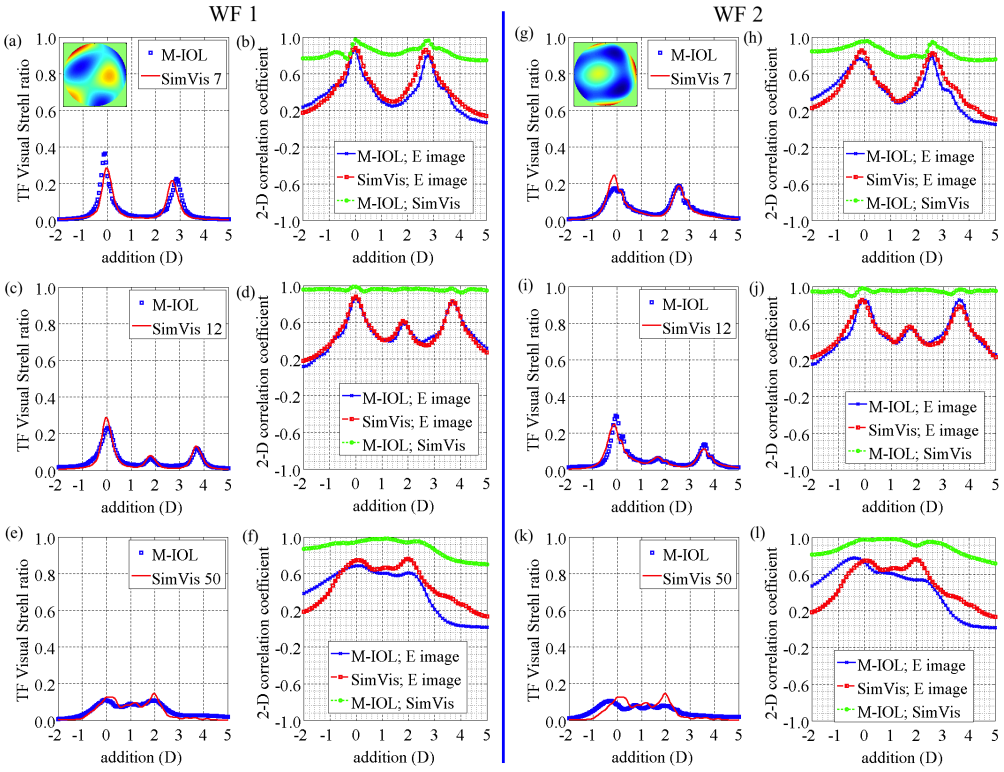

Fig. 8. Effect of aberrations on SimVis: A comparison of TF VS ratio and correlation coefficient for a real-IOL and SimVis in the presence of aberrated wavefronts–WF 1 (a)-(f) and WF 2 (g)-(l)–in the case of segmented bifocal refractive ((a), (b), (g) and (h)), trifocal diffractive ((c), (d), (i) and (j)), and refractive EDOF ((e), (f), (k) and (l)) M-IOLs. SimVis sampling is shown in the subfigure legends.

3.5. *Chromatic aberrations and polychromatic light*

The estimated TF VS ratio for the trifocal diffractive M-IOL at three different wavelengths, 475 nm, 555 nm and 695 nm is shown in Fig. 9(a). The energy distribution varies at far, near and intermediate distances with wavelength [21] and consequently, the corresponding SimVis time coefficients change with the wavelength too. Figure 9(b) shows the estimated polychromatic TF

Biomedical Optics EXPRESS

Table 1. RMS of the two TF optical quality metrics (VS ratio and correlation coefficient) obtained between the profiles of real M-IOLs and SimVis with simulated wavefront aberrations.

M-IOL	*Metric*	*WF 1*	*WF 2*	*20 WFs*
Trifocal diffractive	VS ratio	0.02	0.02	0.02 ± 0.01
Trifocal diffractive	Correlation	0.03	0.05	0.04 ± 0.01
Bifocal refractive	VS ratio	0.04	0.02	0.03 ± 0.01
Bifocal refractive	Correlation	0.09	0.09	0.09 ± 0.01
Refractive EDOF	VS ratio	0.02	0.03	0.03 ± 0.01
Refractive EDOF	Correlation	0.08	0.11	0.12 ± 0.03

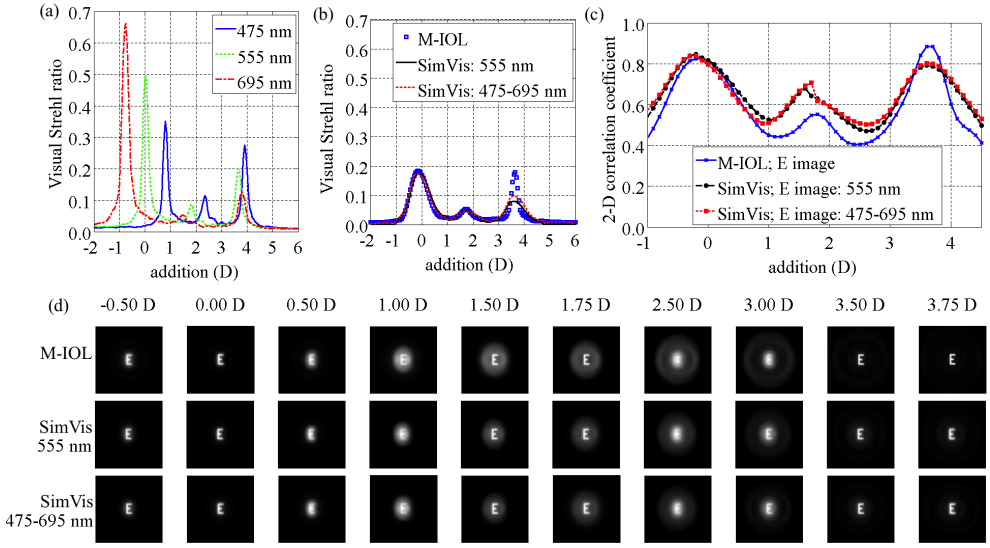

Fig. 9. (a) Monochromatic TF VS ratio curves for the trifocal diffractive M-IOL at three different wavelengths: 475 nm, 555 nm, and 695 nm. (b) A comparison of the polychromatic TF VS ratio for the trifocal diffractive M-IOL and the corresponding SimVis with monochromatic time coefficients (555 nm) or polychromatic time coefficients. (c) A comparison of the 2-D correlation between the nominal 'E' image and the polychromatic TF simulated images. Images were obtained with either the real M-IOL or the SimVis profile (monochromatic or polychromatic time coefficients). (d) The polychromatic TF simulated images obtained with the M-IOL and the SimVis (monochromatic or polychromatic time coefficients).

VS ratio (blue squares) for the trifocal diffractive M-IOL. The polychromatic time coefficients for white light conditions were obtained by using polychromatic TF VS ratio metric for the M-IOL and all the monofocal IOLs possible with a tunable lens in Eq. (3). The TF VS ratio for SimVis (red dotted line) that uses the resultant polychromatic time coefficients is also shown in Fig. 9(b). In comparison, the use of monochromatic time coefficients (at 555 nm) in SimVis (black line) with white light resulted in lower accuracy. Figure 9(c) shows the corresponding 2-D correlation coefficient obtained from the polychromatic TF simulated images (a few examples are shown in Fig. 9(d)).

The broadening of the far peak in SimVis is due to the eye's chromatic aberration, which is similar to the far peak with the trifocal diffractive M-IOL. However, the eye's LCA (with SimVis) also broadens the peak at near, while the trifocal diffractive M-IOL compensates the LCA at near,

Biomedical Optics EXPRESS

the SimVis does not compensate that with the time coefficients.

3.6. Effects of the dynamic behavior of the tunable lens

There is a finite response time (usually lower than a single SimVis cycle) for changing the optical power of the tunable lens. A theoretical analysis was performed to quantify the effects of these temporal dynamics on a pure bifocal IOL design with equal energy at far (0 D: 50%) and near (3 D: 50%) distances. The temporal step response function was modeled using the damped harmonic oscillator shown in Fig. 10(a). The corresponding time coefficients for a pure bifocal IOL with and without the dynamic effects are shown in Fig. 10(b), which is obtained as a histogram of Fig. 10(a). A comparison of the evaluated TF VS ratio profiles with and without the dynamics is shown in Fig. 10(c). A drop in the optical quality is seen with the inclusion of the settling time of the tunable lens.

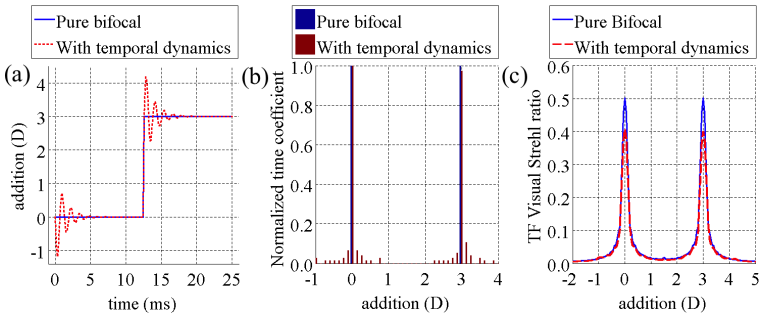

Fig. 10. (a) A single SimVis cycle with and without induced response delay (damped harmonic oscillator). (b) The effective time coefficients with and without the temporal dynamics of the tunable lens. (c) Comparison of the TF VS ratio with and without the inclusion of SimVis temporal dynamics.

4. Discussion

The proposed metric-based method of evaluating the SimVis (based on the tunable lens) time coefficients is effective in replicating the TF optical quality of any given multifocal phase pattern, including in the case of a rotationally asymmetric segmented design. It was found that temporal sampling plays a vital role and the optimal temporal sampling can be determined by using the local optima in the defined relative error metrics based on TF VS ratio and TF image correlation. A reduced sampling in Fig. 1(e) causes inaccuracies at certain distances (for instance, at 1.00 D). However, these errors can be avoided by increasing the sampling from $n_{SimVis} = 12$ to $n_{SimVis} = 25$.

The number of nonzero time coefficients is the largest for the refractive EDOF M-IOL (116) and hence the chosen sampling must be greater than this number. Also, to employ a sampling resolution with exactly two significant digits (0.05 D), 161 sampling points were chosen in the range -2 D and 6 D. In order to undersample the evaluated time coefficients, thresholding was directly applied to refractive EDOF M-IOLs. In the case of M-IOLs with distinct TF optical quality peaks, prior to the application of thresholding, the sampling locations at far, near and intermediate distances were sampled first. This was done to avoid the exclusion of low energy intermediate or near additions when the chosen sampling is low (see Fig. 4). When undersampling without a priori knowledge of the energy distribution, in certain cases, SimVis incorrectly simulates a monofocal IOL, especially when undersampled with fewer nonzero time coefficients.

As sampling increases, the relative error, $\tilde{c}$, increases in the case of segmented bifocal refractive M-IOL (see the red line in Fig. 4(b)). The SimVis time coefficients were evaluated using the

Biomedical Optics EXPRESS

TF VS ratio (that includes the contrast sensitivity function) and not the TF image correlation coefficients (evaluated from the PSFs). Further, the asymmetric geometry and the transition region between and far and near portions of the segmented bifocal refractive M-IOL result in a lower image correlation (c) in comparison with SimVis image correlation (c_s) beyond the near peak and in intermediate distances as observed in Fig. 2(e). As sampling increased, the value of $\tilde{c}$ beyond the near peak increased nearly linearly in the sampling range studied.

In bifocal/trifocal angularly-segmented refractive or pure diffractive M-IOLs with distinct TF optical quality peaks, the effects of pupil size variations are minimal (see Figs. 6(e), 6(f), 7(a) and 7(b)) or can be compensated by increasing the SimVis temporal sampling. While simulating certain M-IOLs including refractive radially-segmented M-IOLs and EDOF lenses, the metric-based SimVis time coefficients are greatly dependent on the pupil size. In EDOF M-IOLs, an increase in sampling is not sufficient to compensate errors due to pupil size variations. Total compensation is possible by precomputing the SimVis time coefficients for different pupil sizes evaluated from the multifocal phase map starting from a minimum pupil size to a large pupil size in small steps. This step resolution required for accurate representation of the M-IOL is dependent on its multifocal phase pattern.

In trifocal diffractive and bifocal refractive M-IOLs, the wavefront aberrations of the eye had a little or negligible effect on the performance of SimVis. In the case of EDOF M-IOLs, the wavefront aberrations of the eye have a complex effect on SimVis. Most EDOF M-IOLs have an aspheric base structure, which causes radially symmetric Zernike polynomial coefficients (no angular variability) in its phase map. The dominant terms include primary defocus, primary spherical and other higher-order spherical polynomial terms. Addition or subtraction of any of these terms due to the presence of wavefront aberrations of the eye affects the replication of the TF optical quality using SimVis. Hence, when simulating EDOF M-IOLs using SimVis, it is important to include the effects of aberrations in the evaluation of the time coefficients, although not yet completely practical in compact clinical devices. A statistically significant positive correlation ($p<0.002$) was observed between the absolute magnitude of spherical aberration in the wavefront aberrations of the simulated wavefronts and the RMS of the difference in TF VS ratio values evaluated between the real M-IOL subjected to 20 different aberrations and SimVis subjected to the same aberrations. Since WF 2 has a higher spherical aberration coefficient in comparison with WF 1, the RMS error in the difference of the TF VS ratio between the real M-IOL with aberrations and corresponding SimVis with aberrations is higher in the case of WF 2 for the refractive EDOF M-IOL case. For exact TF calculation, the effects of aberrations would be incorporated in the evaluation of the time coefficients. However, it was found that typical anomalies could be largely compensated with adjustments to the SimVis temporal profiles.

Optimal sampling is dependent on the TF VS ratio profile. With the inclusion of the wavefront aberrations, the TF VS ratio profile broadens and the TF VS ratio peaks (at far, near and intermediate distances) drop and are also displaced in many cases. As a result, the optimal sampling changes too. The RMS values in Table 1 use the optimal sampling estimated in the absence of aberrations in the case of segmented bifocal refractive and trifocal diffractive M-IOLs. The use of optimal sampling in the presence of aberrations may further reduce the RMS values shown in Table 1.

The polychromatic TF VS ratio curve in Fig. 9(b) for the trifocal diffractive M-IOL is broader at the far distance in comparison with the monochromatic TF VS ratio curves in Fig. 9(a). However, the broadening is negligible at near distance. This is due to the compensation of refractive LCA by the diffractive LCA, both of which take opposite signs with respect to one another at near focus. Since the SimVis time coefficients are evaluated using a broader monofocal TF VS ratio curve, the evaluated polychromatic time coefficients do not accurately replicate the near peak for the trifocal diffractive M-IOL in white light. In the case of M-IOLs with refractive LCA alone, the polychromatic SimVis time coefficients accurately replicate the TF optical quality of the

Biomedical Optics EXPRESS

M-IOL with broad spectrum sources.

The settling time of the tunable lens affects the intended SimVis TF optical quality. The theoretical model presented here estimates the degradation due to this dynamic effect. In Fig. 10, a large amplitude of the damped oscillator (producing an overshoot of more than 1 D) was chosen to illustrate the effect. However, in practice, a small amplitude is expected, which increases linearly with increasing addition step. The dynamic effects can be corrected by measuring the temporal step response function of the tunable lens using fast focimetry. A correction signal (obtained by inverting the dynamic artifacts) can be programmed in SimVis to obtain the desired TF optical quality.

A high degree of the lens opacity may limit the applicability of simultaneous vision simulators in cataracts. The overall degradation in the light level due to a loss in transparency is the same in spatial [4] or temporal (SimVis) simultaneous vision simulators. However, while replicating refractive multifocal designs with the spatial simultaneous vision simulators, opacities may unevenly obstruct far and near portions of the multifocal pupillary distribution. Hence, the distribution of the opacities across the pupil affects the accuracy of spatially simulating the intended energy distribution. In contrast, the temporal multiplexing nature of the SimVis device produces far or near corrections across the entire pupil at any given point of time. The time-multiplexed simultaneous vision image is projected onto the retina through the clear portions of the lens. Therefore, temporal multiplexing with SimVis is advantageous over spatial simulators of refractive multifocal designs in the presence of cataract with significant occlusion.

In the future, a direct comparison between the real M-IOLs and the SimVis device with the help of psychophysical measurements in a custom adaptive optics system can offer further evidence to the theoretical validation of the evaluated SimVis temporal profile.

5. Conclusions

In summary, a new metric-based approach is proposed that allows simulating any given M-IOL using temporal multiplexing in a tunable lens. The effect of temporal sampling, wavelength, pupil size variations, wavefront aberrations of the eye, chromatic aberrations of the M-IOL and temporal dynamics of the tunable lens were investigated. The proposed method was implemented in three M-IOLs. Along with the possibility of comparing across lens designs in the presence of cataract, the instrument holds great promise for early, mid-stage cataracts and non-cataract presbyopes considering multifocal lens exchange. The device can easily be extended to simulate multifocal contact lenses. A routine trial and error procedure of choosing a multifocal contact lens is usually lengthy and exhausting. The SimVis instrument has the potential to simplify the whole process.

Funding

Consejería de Educación, Juventud y Deporte of Comunidad de Madrid and the People Programme (Marie Curie Actions) of the European Union's Seventh Framework Programme (FP7/2007-2013) under REA grant agreement (n° 291820); Ministerio de Economía y Competitividad (DTS16-00127); Spanish Government Torres-Quevedo Program (PTQ-15-07432); EIT Health e.V. Grant agreement (HS-2016-SPAIN-03); ERC Grant Agreement (ERC-2011-AdC 294099); Spanish Government Grant (FIS2014-56643-R).

Disclosures

VA: 2Eyes Vision S. L. (I), CD: 2Eyes Vision S. L. (I,P), EG: 2Eyes Vision S. L. (I,E), SM: 2Eyes Vision S. L. (I,P).